Available online at www.sciencedirect.com
SCIENCE DIRECT®
Journal of Solid State Chemistry 178 (2005) 3740–3746
JOURNAL OF SOLID STATE CHEMISTRY
www.elsevier.com/locate/jssc

Hybrid inorganic–organic 1-D and 2-D frameworks with $\{As_8V_{14}O_{42}\}$ clusters as building blocks

Shou-Tian Zheng[a], Jie Zhang[a], Ji-Qing Xu[b], Guo-Yu Yang[a,c,*]

[a]*State Key Laboratory of Structural Chemistry, Fujian Institute of Research on the Structure of Matter, Chinese Academy of Sciences, Fuzhou, Fujian 350002, China*
[b]*College of Chemistry and State Key Laboratory of Inorganic Synthesis and Preparative Chemistry, Jilin University, Changchun, Jilin 130023, China*
[c]*State Key Laboratory of Coordination Chemistry, Nanjing University, Nanjng, Jiangsu 210093, China*

Received 4 June 2005; received in revised form 15 September 2005; accepted 17 September 2005
Available online 20 October 2005

Abstract

Three novel hetero-polyoxovanadates, $[Cd(2,2'\text{-bpy})_3]\{[Cd(dien)]As_8V_{14}O_{42}(H_2O)\}$ (**1**, 2,2′-bpy = 2,2′-bipyridine, and dien = diethylenetriamine), $[Zn(2,2'\text{-bpy})_2]_2[As_8V_{14}O_{42}(H_2O)]\cdot H_2O$ (**2**) and $[Ni(en)_2]_3[As_8V_{14}O_{42}(HPO_3)]\cdot 4H_2O$ (**3**, en = ethlenediamine), were hydrothermally synthesized and characterized by single-crystal X-ray diffraction. Crystal data: **1** monoclinic, $P2(1)/n$, $a = 15.1728(5)$, $b = 19.2863(5)$, $c = 25.7122(9)$ Å, $\beta = 96.005(2)^\circ$, $Z = 4$. **2**, orthorhombic, $P2(1)2(1)2(1)$, $a = 12.1270(3)$, $b = 15.8678(8)$, $c = 40.0422(1)$ Å, $Z = 4$. **3**, triclinic, $P\bar{1}$, $a = 12.9340(3)$, $b = 13.4130(3)$, $c = 21.1820(4)$ Å, $\alpha = 87.170(3)^\circ$, $\beta = 77.517(3)^\circ$, $\gamma = 68.480(3)^\circ$, $Z = 2$. Compounds **1–3** are all made of the $\{As_8V_{14}O_{42}\}$ shells linked by corresponding transition metal complexes into extended structures. Compound **1** and **2** present 1-D wave-like and tubular structures, respectively, while compound **3** exhibits a novel 2-D structure containing interwinding puckery layers. Variable temperature susceptibility measurements demonstrate the presence of antiferromagnetic interaction between V^{IV} cations in **1** and **2**.

Keywords: Polyoxometalate; Vanadium; Arsenic; Metal-oxygen cluster; Crystal structure; Hydrothermal synthesis

1. Introduction

Owing to their exceptional ability to form mixed-valence compounds that exhibit rich electronic and magnetic properties, polyoxometalates (POMs) have been extensively studied with lots of structurally characterized examples now known [1]. However, most of POMs are discrete structures. Now, one of the challenging tasks in POMs chemistry is to find some bridging units and then link POMs building units up into extended frameworks, which is of great interest not only from a structural point of view but also because they are potentially interesting for applications in different areas such as catalysis, electrical conductivity, and biological chemistry [2]. On-going research has demonstrated that transition metal (e.g. Fe, Co, Ni, Cu, Zn and Mn) coordination complexes may serve as inorganic bridging ligands linking POM clusters into 1-D, 2-D and 3-D networks [3–8], such as $[H_2en]_2[\{Cu(en)(OH_2)\}Mo_5P_2O_{23}]\cdot 4H_2O$ [6], $[\{Co(en)_2\}_2Sb_8V_{14}O_{42}(H_2O)]\cdot 6H_2O$ [7], $[SiW_{11}O_{39}Ni(4,4'\text{-bpy})][Ni(4,4'\text{-Hbpy})_2(H_2O)_2]\cdot(4,4'\text{-}H_2bpy)\cdot 6H_2O$ [8]. In particular, Zubieta et al. have reported a series of novel materials consisting of Mo–O clusters attached various transition metal complexes [9–12]. Typical examples include $[Ni(2,2\text{-bpy})_2Mo_4O_{13}]$ [10], a 1-D chain, $[\{Cu_3(4,7\text{-phen})_3\}_2\{Mo_{14}O_{45}\}]$ [11], a 2-D framework, and $[\{Fe(tpyor)\}_3Fe(Mo_6O_{19})_2]\cdot XH_2O$ [12], which has a 3-D framework. In addition, Khan et al., have also prepared a series of novel framework materials composed of molecular vanadium oxide clusters linked by $[M(H_2O)_4]^{2+}$ (M = Mn, Fe, Ni, Zn, Co, Cd) units [13]. The successful syntheses of these materials demonstrate that some control is achievable in defining their structures.

*Corresponding author. State Key Laboratory of Structural Chemistry, Fujian Institute of Research on the Structure of Matter, Chinese Academy of Sciences, Fuzhou, Fujian 350002, China. Fax: +86 591 8371 0051.
E-mail address: ygy@fjirsm.ac.cn (G.-Y. Yang).

0022-4596/$ - see front matter © 2005 Elsevier Inc. All rights reserved.
doi:10.1016/j.jssc.2005.09.029

Of the large POMs family, an important subclass is arsenic–vanadium clusters with arsenic and vanadium in low oxidation states, which often act as cryptates encapsulating neutral molecules or anions. To date, although a number of arsenic–vanadium clusters have been synthesized [14,15], the linking of arsenic–vanadium clusters into extended structures is very rare [16]. Therefore, the synthesis of extended solids based on arsenic–vanadium clusters in the presence of transition metal complexes is a rewarding challenge. In this article, we describe the hydrothermal synthesis and structural characterization of the following three novel extended POMs based on $\{As_8V_{14}O_{42}\}$ clusters as building blocks, $[Cd(2,2'\text{-bpy})_3]\{[Cd(dien)]As_8V_{14}O_{42}(H_2O)\}$ (**1**), $[Zn(2,2'\text{-bpy})_2]_2[As_8V_{14}O_{42}(H_2O)]\cdot H_2O$ (**2**) and $[Ni(en)_2]_3[As_8V_{14}O_{42}(HPO_3)]\cdot 4H_2O$ (**3**).

2. Experimental section

2.1. General methods

All chemicals purchased were of reagent grade and used without further purification. Elemental analyses were determined on a PE 2400 II elemental analyzer. IR spectra (KBr pellets) were recorded on an ABB Bomen MB 102 spectrometer. EPR spectra were carried out on powder samples at X-band frequency with a Bruker ER-420 spectrometer at room temperature. Reactions were carried out in 40 ml Teflon-lined steel autoclave at autogenous pressure. Variable temperature susceptibility measurements were carried out in the temperature range 2–300 K at a magnetic field of 1 T on polycrystalline samples with a SQUID MPMS-7 magnetometer manufactured by Quantum Design. Background corrections for the sample holder assembly and diamagnetic components of the compound were applied.

2.2. Synthesis

2.2.1. Synthesis of $[Cd(2,2'\text{-bpy})_3][\{Cd(dien)\}As_8V_{14}O_{42}(H_2O)]$ (*1*)

A mixture of V_2O_5 (0.30 g, 1.65 mmol), As_2O_3 (0.33 g, 1.67 mmol), $3CdSO_4\cdot 8H_2O$ (0.42 g, 1.64 mmol), 2,2′-bpy (0.50 g, 3.21 mmol), $H_2C_2O_4\cdot 2H_2O$ (0.21 g, 1.67 mmol), dien (0.30 mL) and H_2O (20 mL, 1.11 mol) was heated at 160 °C for 3 days and then cooled to room temperature. The product was isolated as brown blocks (51.3% yield based on V). Anal. Calcd for $C_{34}H_{39}N_9O_{43}As_8Cd_2V_{14}$: C, 14.58; H, 1.40; N, 4.50 wt%. Found: C, 14.52; H, 1.54; N, 4.43 wt%. IR (KBr, cm^{-1}) for **1**: 1599s, 1491w, 1475m, 1438s, 1358w, 1313w, 1249w, 1157w, 1116w, 995s, 822m, 762s, 714s, 629s, 557m, 468s.

2.2.2. Synthesis of $[Zn(2,2'\text{-bpy})_2]_2[As_8V_{14}O_{42}(H_2O)]\cdot H_2O$ (*2*)

A mixture of V_2O_5 (0.20 g, 1.10 mmol), As_2O_5 (0.30 g, 1.30 mmol), $Zn(CH_3COO)_2\cdot 2H_2O$ (0.30 g, 1.37 mmol), 2,2′-bpy (0.20 g, 1.28 mmol), tetramethylammonium hydroxide solution (0.1 g, 25 wt%) and H_2O (8 mL, 0.44 mol) was heated at 160 °C for 6 days and then cooled to room temperature. The product was isolated as brown blocks (33.1% yield based on V). Anal. Calcd for $C_{40}H_{36}N_8O_{44}As_8V_{14}Zn_2$: C, 17.29; H, 1.31; N, 4.03 wt%. Found: C, 17.17; H, 1.39; N, 3.95 wt%. IR (KBr pellet ν/cm^{-1}) for **2**: 1593(s), 1471(m), 1441(s), 1311(m), 992(s), 954(s), 763(s), 702(s), 626(s), 558(m), 459(s), 405(w).

2.2.3. Synthesis of $[Ni(en)_2]_3[As_8V_{14}O_{42}(HPO_3)]\cdot 4H_2O$ (*3*)

A mixture of V_2O_5 (1.01 g, 5.55 mmol), As_2O_3 (0.83 g, 4.19 mmol), H_3PO_3 (1.71 g, 16.76 mmol), en (0.19 mL), Ni (0.20 g, 3.45 mmol), $Ni(CH_3COO)_2\cdot 4H_2O$ (0.52 g, 2.03 mmol) and H_2O(10 mL, 0.56 mol) was heated at 160 °C for 4 days and then cooled to room temperature. The product was isolated as brown blocks (16.3% yield based on V). Anal. Calcd for $(C_{12}H_{58}N_{12}O_{51}PAs_8V_{14}Ni_3)$: C, 5.32; H, 2.16; N, 6.21 wt%. Found: C, 5.06; H, 2.21; N, 5.83 wt%. IR (KBr, cm^{-1}) for **4**: 1570(s), 1480(m), 1380(m), 1310(m), 1203(w), 996(s), 951(s), 758(s), 611(m), 457(m).

2.3. X-ray crystallography

X-ray data were collected at room temperature on a Rigaku Mercury CCD/AFC diffractometer with MoK_α radiation ($\lambda = 0.71073$ Å). Lorentz and polarization corrections as well as empirical absorption correction were carried out for the net intensities [17]. The structures were solved by direct methods and refined by full-matrix least-squares techniques using SHELXTL97 [18]. All non-hydrogen atoms were treated anisotropically in the three complexes. No attempt was made to locate the hydrogen atoms of water. The Flack parameter (−0.007(15)) for **2** indicates the correct absolute configuration. The crystallographic data are summarized in Table 1. Ranges of selected bond distances of **1**–**3** are listed in Table 2. CCDC-254403, 242420 and 259394 contain the supplementary crystallographic data for this paper. These data can be obtained free of charge via www.ccdc.cam.ac.uk/conts/retrieving.html [or from the Cambridge Crystallographic Data Centre, 12, Union Road, Cambridge CB2 1EZ, UK; fax: (internat.) +44 1223 336 033; or deposit@ccdc.cam.ac.uk].

3. Result and discussion

The $\{As_8V_{14}O_{42}\}$ shells in **1**–**3** are essentially identical with the $\{As_8V_{14}O_{42}\}$ shells in the fully reduced anions $[As_8V_{14}O_{42}(X^{n-})]^{(4+n)-}$ ($X = SO_4^{2-}$, SO_3^{2-}, $0.5H_2O$) [14d,15a]. Here, we use the $\{As_8V_{14}O_{42}\}$ shell in **1** as an example to describe its structure in detail. As shown in the Fig. 1, the $\{As_8V_{14}O_{42}\}$ shell consists of 14 condensed vanadium oxygen square pyramids (VO_5) and 8 trigonal pyramids (AsO_3). Two AsO_3 groups are joined together by an oxygen

Table 1
Crystallographic data for compounds **1–3**

Compound	**1**	**2**	**3**
Formula	$C_{34}H_{39}N_9O_{43}As_8Cd_2V_{14}$	$C_{40}H_{36}N_8O_{44}As_8V_{14}Zn_2$	$C_{12}H_{58}N_{12}O_{51}PAs_8V_{14}Ni_3$
M_r	2799.06	2776.03	2706.32
Crystal system	Monoclinic	Orthorhombic	Triclinic
Space group	$P2(1)/n$	$P2(1)2(1)2(1)$	$P\bar{1}$
Crystal size (mm)	$0.48 \times 0.38 \times 0.30$	$0.32 \times 0.24 \times 0.20$	$0.20 \times 0.24 \times 0.48$
a (Å)	15.1728(5)	12.1270(3)	12.9340(3)
b (Å)	19.2863(5)	15.8678(3)	13.4130(3)
c (Å)	25.7122(9)	40.0422(1)	21.1820(4)
α	90	90	87.170(3)
β (deg)	96.005(2)	90	77.517(3)
γ	90	90	68.480(3)
V (Å^3)	7482.8(4)	7705.3(2)	3335.94(12)
Z	4	4	2
D_c (g cm^{-3})	2.485	2.393	2.694
μ (mm^{-1})	5.822	5.729	6.760
Reflections collected	55359	19076	7252
Unique data (R_{int})	16662(0.0259)	13110(0.045)	5742(0.0389)
F (000)	5328	5320	2614
Θ range (deg)	3.08–27.48	2.61–25.05	1.63–25.00
Goodness of fit	1.061	1.244	1.056
R_1, wR_2 [$I>2\sigma(I)$][a]	0.0314, 0.0733	0.0655, 0.1225	0.0461, 0.1179
$\Delta\rho_{max}$, $\Delta\rho_{min}$ (eÅ^{-3})	1.727, −2.081	1.337, −0.836	0.809, −0.776

[a] $R_1 = \sum ||F_o|-|F_c|| / \sum |F_o|$; $wR_2 = \{\sum[w(F_o^2-F_c^2)^2] / \sum[w(F_o^2)^2]\}^{1/2}$.

Table 2
Ranges of some important bond lengths (Å) for compounds **1–3**[a]

1			
V=O$_t$	1.592(2)–1.637(2)	Cd$_1$–N	2.271(5)–2.314(4)
V–O$_b$	1.905(2)–2.021(2)	Cd$_2$–N	2.262(3)–2.399(3)
As–O	1.759(2)–1.790(2)	Cd$_1$–O	2.231(2)–2.258(2)
2			
V=O$_t$	1.529(11)–1.634(9)	Zn$_2$–N	2.122(11)–2.183(13)
V–O$_b$	1.890(9)–2.028(10)	Zn$_1$–O	2.081(9)–2.154(10)
As–O	1.735(11)–1.821(10)	Zn$_2$–O	2.025(9)–2.138(9)
Zn1–N	2.128(11)–2.173(12)		
3			
V=O$_t$	1.581(9)–1.632(9)	Ni$_4$–N	1.920(14)–1.954(12)
V–O$_b$	1.901(8)–2.693(19)	Ni$_1$–O	2.101(10)
As–O	1.746(9)–1.795(8)	Ni$_2$–O	2.096(8)–2.123(8)
Ni$_1$–N	2.080(10)–2.105(10)	Ni$_3$–O	2.093(8)
Ni$_2$–N	2.045(11)–2.096(10)	Ni$_4$–O	2.027(11)
Ni$_3$–N	2.078(10)–2.078(13)	P–O	1.411(16)–1.559(18)

[a] O$_t$, terminal oxygen atoms; O$_b$, oxygen atoms in basal plane of VO_5 pyramids.

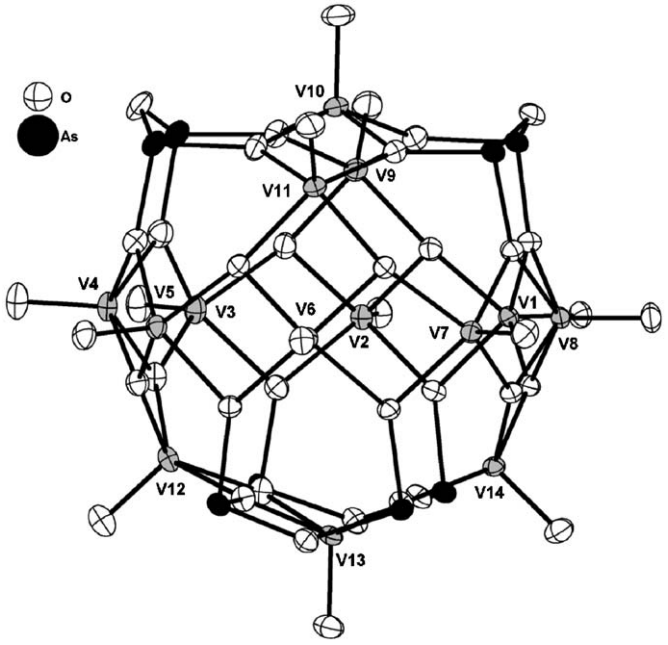

Fig. 1. Structure of $\{As_8V_{14}O_{42}\}$ shell in **1**, with 50% thermal ellipsoids.

bridge, forming a handle-like As_2O_5 moiety. Eight VO_5 (V1, V2, V3, V4, V5, V6, V7, V8) square pyramids share their edges of the base to form a ring. In addition, other six VO_5 (V9, V10, V11, V12, V13, V14) square pyramids share their edges to form two trimers. One trimer is connected across the ring by sharing edges with two VO_5 (V2, V6) square pyramids in the V_8O_{24} ring. The other trimer is similarly connected on the opposite side of the V_8O_{24} ring to the other two VO_5 (V4, V8) square pyramids. The remaining four square faces are formed by the bases of the As_2O_5 units to give a total anion composition of $\{As_8V_{14}O_{42}\}$ shell. In compounds **1–3**, all of the VO_5 square pyramids have typical geometries with apical and basal VO bond distances in the ranges 1.529(11)–1.637(2) Å and 1.890(9)–2.041(9) Å, respectively, and in the As_2O_5 fragments, all the As–O distances are in the ranges 1.735(11)–1.821(10) Å, all the As–O–As angles of

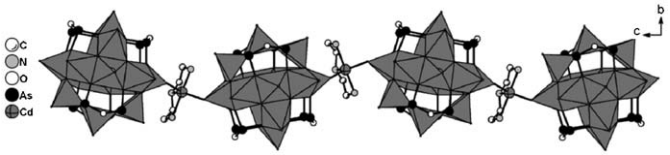

Fig. 2. A view of the chain in **1** showing the connectivity between the $[As_8V_{14}O_{42}(H_2O)]^{4-}$ clusters and $[Cd(dien)]^{2+}$ bridges and orientation of the chain.

130.1(6)–134.2(5)° are bigger than the O–As–O angles of 97.0(4)–101.9(4)°. On the basis of bond valence sum ($\sum_s$) calculations [19] in **1–3**, the oxidation states of all V atoms are +4 ($\sum_s = 4.04$–4.11, **1**; $\sum_s = 4.06$–4.35, **2**; $\sum_s = 3.92$–4.14, **3**) and the As atoms are +3 ($\sum_s = 3.04$–3.12, **1**; $\sum_s = 3.03$–3.24, **2**; $\sum_s = 3.09$–3.32, **3**). The oxidation states of the V and the As atoms are consistent with the formulas of **1–3**. The EPR spectra of **1** and **2** at room temperature show the *g* values are 1.9456 and 1.9493, respectively, corresponding to the signal of V^{4+}. But the EPR spectrum of **3** at room temperature shows no signal for V^{4+}, which indicates that the electrons of the cluster are spin–spin coupled.

Compound **1** consists of anionic chains $\{[Cd1(dien)]As_8V_{14}O_{42}(H_2O)\}^{2-}$ and isolated cations $[Cd2(2,2'\text{-bpy})_3]^{2+}$ occupying the interchain regions and providing charge compensation (Figure S1). The structure of anionic chain $\{[Cd1(dien)]As_8V_{14}O_{42}(H_2O)\}^{2-}$ can be seen in Fig. 2, each two $[As_8V_{14}O_{42}(H_2O)]^{4-}$ clusters link each other by one μ_2-$[Cd1(dien)]^{2+}$ bridge through terminal oxygen groups of two pyramidal V sites in the V_8O_{24} ring with O–Cd1–O angle of 101.70(8)° and Cd1–O distances of 2.231(2) and 2.258(2) Å to form infinite wave-like chain. The Cd1–N1, Cd1–N2 and Cd1–N3 distances are 2.314(4), 2.271(5) and 2.288(4) Å, respectively, which are comparable with the values observed in compound Cd $[C_3N_2H_{11}]_2[V_8O_{20}]$ [20]. The pattern of bond lengths and angles about the five-coordinate cadmium center is best described as a distorted trigonal bipyramidal configuration, with the atoms N1 and N3 occupying the axial positions. As shown in Fig. 3, the $\{[Cd1(dien)]As_8V_{14}O_{42}(H_2O)\}^{2-}$ chains are aligned parallel to the *c*-axis and separated by charge compensatory cations $[Cd2(2,2'\text{-bpy})_3]^{2+}$. It is interesting that the bridging metal atoms and the charge compensatory metal atoms are coordinated by different organic ligands rather than the same ligands in most of reported POMs compounds. The $[Cd2(2,2'\text{-bpy})_3]^{2+}$ cations present both *Δ* and *Λ* enantiomers in **1**. The two kinds of $[Cd2(2,2'\text{-bpy})_3]^{2+}$ chiral enantiomers coexist in every chain regions and give 1:1 molecular proportion. No obvious $\pi-\pi$ interactions are found among $[Cd2(2,2'\text{-bpy})_3]^{2+}$ cations as can be judged by the interring separation of approximately 12.19 Å along the *a*-axis. Thus, these cations and polyoxoanions are contacted with each other mainly through electrostatic interactions.

POMs with helical or chiral structures are of particular interest [6,21]. Single-crystal X-ray diffraction analysis

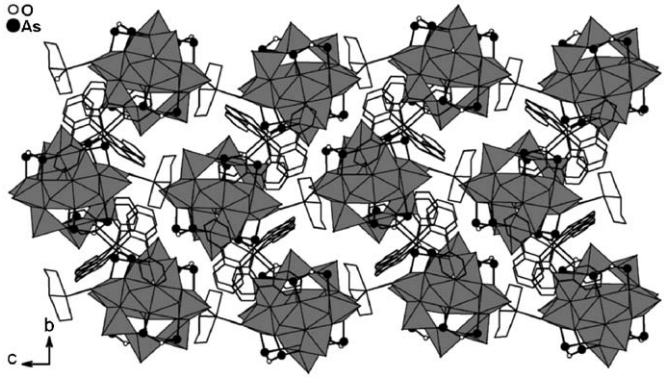

Fig. 3. The packing arrangement of compound **1**, view along the *a*-axis direction.

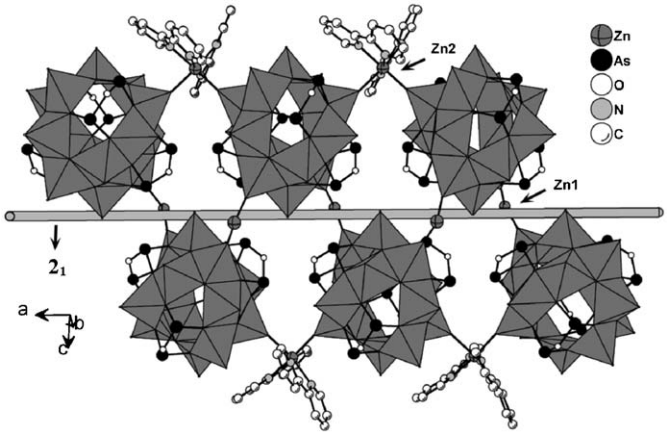

Fig. 4. A view of the chain in **2** showing the connectivity between the $[As_8V_{14}O_{42}(H_2O)]^{4-}$ clusters and $[Zn(2,2\text{-bpy})]^{2+}$ bridges and orientation of the chain.

revealed that compound **2** exhibits a rare 1-D tube-shaped neutral structure constructed from two subunits, namely $\{[Zn1(2,2'\text{-bpy})_2][As_8V_{14}O_{42}(H_2O)]\}_\infty$ helical chain and $[Zn2(2,2'\text{-bpy})_2]^{2+}$ unit (Figure S2). As shown in Fig. 4, the $[As_8V_{14}O_{42}(H_2O)]^{4-}$ clusters are connected through *cis*-$[Zn1(2,2'\text{-bpy})_2O_2]^{2+}$ units via corner-sharing interactions of the type V = O–Zn to form infinite chain, which arranged about a twofold screw axis along *a*-axis and formed a left-handed helical array. Then, the adjacent $[As_8V_{14}O_{42}(H_2O)]^{4-}$ clusters in the left-helical chain are further linked by *cis*-$[Zn2(2,2'\text{-bpy})_2O_2]^{2+}$ units. As a result, 1-D tubular chain is formed. Both crystallographically independent Zn centers adopt octahedral geometry, being coordinated by four nitrogen donors of two 2,2′-bpy with Zn–N distances in the range of 2.122(11)–2.183(13) Å, and two *cis* oxygen atoms from the cluster anion with Zn–O distances in the range of 2.025(9)–2.154(10) Å. As illustrated in Fig. 5, the tubular chains are parallel stacked along *b*-axis to generate chain layers that is parallel to the *ab*-plane, and then these chain layers are further stacked along the *c*-axis in ABAB sequence to form **2**. It is noteworthy that no right-handed helical $\{[Zn1(2,2'\text{-bpy})_2][As_8V_{14}O_{42}(H_2O)]\}_\infty$ subunits are found in **2**.

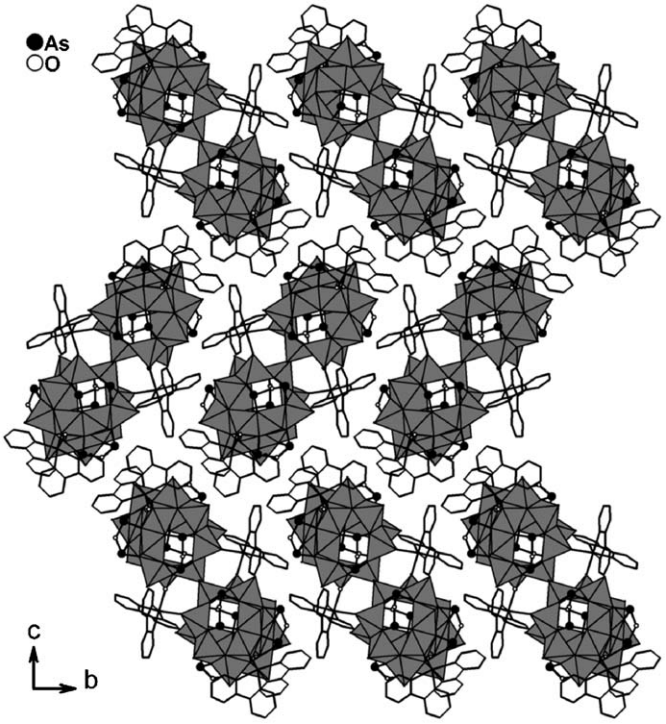

Fig. 5. Packing arrangement of compound **2**, viewed along the *a*-axis direction.

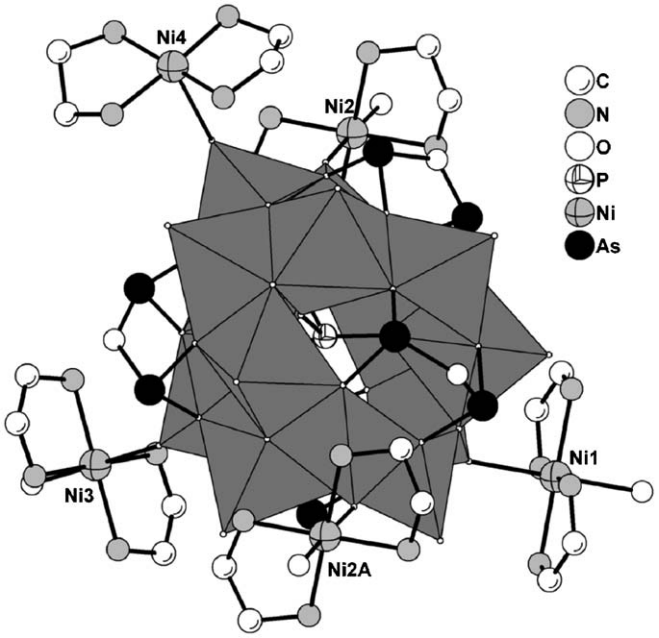

Fig. 6. A view of coordination mode between $[As_8V_{14}O_{42}(HPO_3)]^{6-}$ cluster and $[Ni(en)_2]^{2+}$ units.

The structure of **3** is constructed from linking the $[As_8V_{14}O_{42}(HPO_3)]^{6-}$ clusters and $[Ni(en)_2]^{2+}$ groups into a 2-D network with water molecules occupying the interlayer regions. The structure of the cluster anion may be viewed as a shell of $\{As_8V_{14}O_{42}\}$ encapsulating a $\{HPO_3\}$ moiety. The oxygen atoms of $\{HPO_3\}$ moiety can be divided into two kinds. One is μ_4-bridging oxygen which is covalently bonded to three different vanadium centers via weak ineteractions of μ_4–O–V (2.435(28)–2.693(19) Å). Another is μ_3-bridging oxygen which is covalently bonded to two different vanadium centers with μ_3–O–V distances in the 2.416(21)–2.664(23) Å range. As shown in Fig. 6, each $[As_8V_{14}O_{42}(HPO_3)]^{6-}$ cluster anion bonds to five $[Ni(en)_2]^{2+}$ coordination groups through the bond type Ni–O═V with Ni–O distances in the 2.027(11)–2.123(8) Å range. The $[Ni(en)_2]^{2+}$ coordination units can also be classified into two groups: bridging unit and decorating unit. All bridging Ni centers (Ni1, Ni2 and Ni3) are octahedrally coordinated by four equatorial N atoms from two en ligands and two *trans*-oxo atoms from two neighboring clusters, whereas decorating Ni center (Ni4) adopts a square pyramidal geometry, being coordinated by four N atoms from two en ligands, and one terminal oxygen atom from a cluster. Each $[As_8V_{14}O_{42}(HPO_3)]^{6-}$ cluster is decorated by a $[Ni4(en)_2]^{2+}$ group which is not further connected with other clusters, forming a $[\{Ni4(en)_2\}As_8V_{14}O_{42}(HPO_3)]^{4-}$ anion. Then each two adjacent $[\{Ni4(en)_2\}As_8V_{14}O_{42}(HPO_3)]^{4-}$ anions are bridged by *trans*-$[Ni1(en)_2O_2]^{2+}$ and *trans*-$[Ni3(en)_2O_2]^{2+}$ groups in turn into zigzag chain along the [110] direction, while the *trans*-$[Ni2(en)_2O_2]^{2+}$ groups provide the cross-linking between adjacent chains into a 2-D puckery framework (Fig. 7). The most interesting feature of **3** is that each 2-D puckery layer is interpenetrated by another identical 2-D puckery layer, resulting in a 2-D interwinding architecture which is not observed previously in polyoxovanadate (Fig. 8). These interwinding 2-D architectures are aligned parallel to the *ab*-plane and are stacked along the *c*-axis direction in AAAA sequence to form compound **3** (Figure S3).

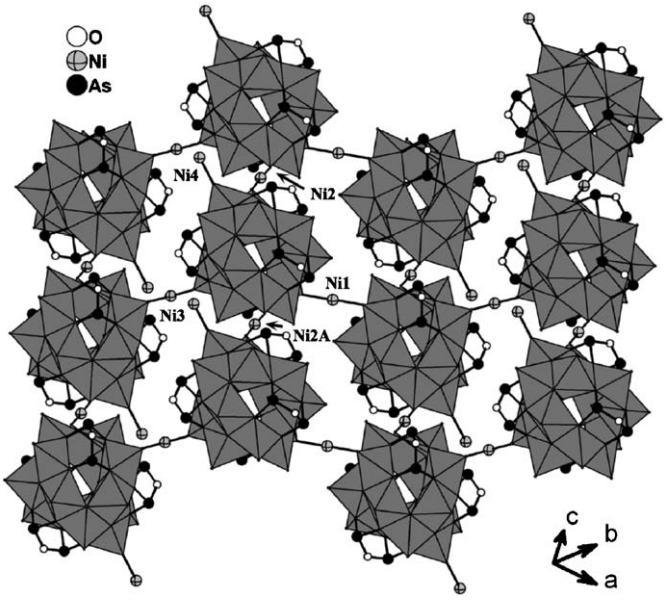

Fig. 7. A view of a portion of a single layer in the structure of **3**. The en ligands and HPO_3^{2-} anions encapsulated in the $\{As_8V_{14}O_{42}\}$ shell have been omitted for clarity.

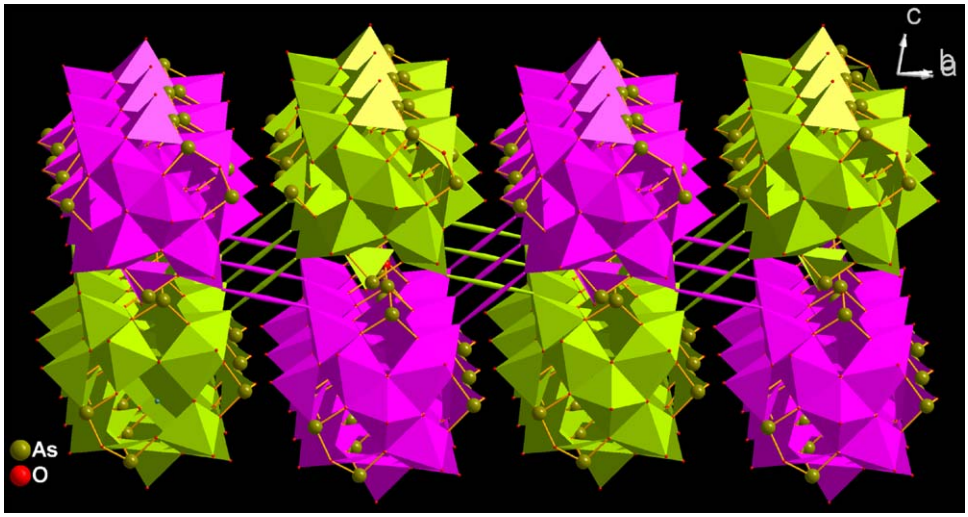

Fig. 8. A view of the 2-D interpenetrable architecture of **3**. The two independent layers are represented by purple polyhedrons and green polyhedrons, respectively.

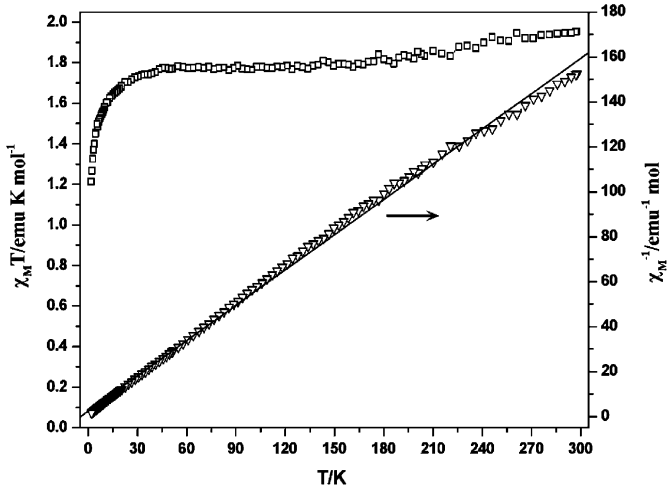

Fig. 9. Temperature dependence of the $\chi_M T$ value and reciprocal susceptibility χ_M^{-1} for **1**.

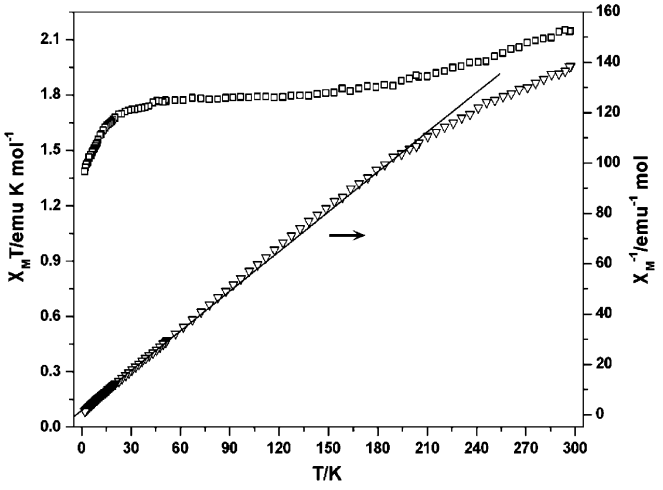

Fig. 10. Temperature dependence of the $\chi_M T$ value and reciprocal susceptibility χ_M^{-1} for **2**.

The variable temperature magnetic susceptibility of **1**and **2** were measured between 2 and 300 K. Fig. 9 and Fig. 10 show the magnetic behavior of **1** and **2** in the form of a reciprocal molar susceptibility (χ_M^{-1}) and $\chi_M T$ vs. temperature, respectively, where χ_M is the molar magnetic susceptibility. The magnetism may be attributed solely to the presence of V^{4+} ions ($3d^1$, $S = 1/2$). The $\chi_M T$ value of the complex **1** at 300 K is 1.95 $cm^3\,K\,mol^{-1}$ (3.95 μ_B), much smaller than that expected for the total spin-only value 4.97 $cm^3\,K\,mol^{-1}$ (6.30 μ_B) of 14 V^{4+} with $S = 1/2$. ($g = 1.9456$ for V^{4+} from EPR result). As the temperature decreases, the $\chi_M T$ value of the complex **1** decreases nearly linearly until 130 K to stabilize approximately at 1.78 $cm^3\,K\,mol^{-1}$ (3.77 μ_B). Below 50 K another faster decrease of $\chi_M T$ is observed, with ca.1.21 $cm^3\,K\,mol^{-1}$ (3.11 μ_B) at 2 K. The temperature-dependences of $\chi_M T$ for **1** demonstrate the existence of antiferromagnetic coupling interaction. This antiferromagnetic character is in agreement with a negative Weiss constant obtained from a linear fitting of χ_M^{-1} vs T ($\theta = -0.21$ K) from 2 to 300 K. For complex **2**, $\chi_M T$ at room temperature is 2.15 $cm^3\,K\,mol^{-1}$ (4.15 μ_B), which is also much lower than the value expected for 14 uncoupled electrons (4.99 $cm^3\,K\,mol^{-1}$, 6.32 μ_B, $g = 1.9493$). Upon cooling from room temperature, the $\chi_M T$ value decreases nearly linearly until 125 K to stabilize approximately at 1.80 $cm^3\,K\,mol^{-1}$ (3.79 μ_B), and then decreases rapidly from 50 K and reaches a minimum value of 1.39 $cm^3\,K\,mol^{-1}$ (3.33 μ_B) at 2 K, suggesting an antiferromagnetic coupling between vanadium centers. The magnetic suseptibility obeys the Curie–Weiss law in the range of 2–210 K, giving a Weiss constant $\theta = -0.13$ K and a Curie constant $C = 0.41$ $cm^3\,K\,mol^{-1}$. The temperature-dependences of $\chi_M T$ for **1** and **2** demonstrate the existence of antiferromagnetic coupling interaction, which is a

common feature for most poly oxovanadate culsters [22,23]. Because no suitable theoretical model is available in the literature for such a complex system [24], detailed magnetic analyses were not done for the present compounds.

Appendix A. Supplementary Materials

Supplementary data associated with this article can be found in the online version at doi:10.1016/j.jssc.2005.09.029.

References

[1] (a) M.T. Pope, A. Müller, Angew. Chem. Int. Ed. Engl. 30 (1991) 34;
(b) M.T. Pope, Heteropoly and Isopoly Oxometalates, Springer, Berlin, 1983.
[2] D.E. Katsoulis, Chem. Rev. 98 (1998) 359.
[3] J.R.D. DeBord, R.C. Haushalter, L.M. Meyer, D.J. Rose, P.J. Zapf, J. Zubieta, Inorg. Chim. Acta. 256 (1997) 165.
[4] M.I. Khan, E. Yohannes, R.J. Doedens, Inorg. Chem. 42 (2003) 3125.
[5] J. Lu, E.H. Shen, M. Yuan, Y.G. Li, E.B. Wang, C.W. Hu, L. Xu, J. Peng, Inorg. Chem. 42 (2003) 6956.
[6] Y. Xu, N. Goh, L. Chia, Chem. Commun. (1998) 1709.
[7] L.J. Zhang, X.L. Zhao, J.Q. Xu, T.G. Wang, J. Chem. Soc. Dalton Trans. (2002) 3275.
[8] P.Q. Zheng, Y.P. Ren, L.S. Long, R.B. Huang, L.S. Zheng, Inorg. Chem. 44 (2005) 1190.
[9] (a) D. Hagrman, R.C. Haushalter, J. Zubieta, Chem. Mater. 10 (1998) 361;
(b) R.L. Laduca, R. Finn, J. Zubieta, Chem. Commun. (1999) 1669;
(c) P.J. Hagrman, D. Hagrman, J. Zubieta, Angew. Chem. Int. Ed. 38 (1999) 2638.
[10] P.J. Zapf, C.J. Warren, R.C. Haushalter, J. Zubieta, Chem. Commun. (1997) 1543.
[11] D. Hagrman, P.J. Zapf, J. Zubieta, Chem. Commun. (1998) 1283.
[12] D. Hagrman, P.J. Hagrman, J. Zubieta, Angew. Chem. Int. Ed. 38 (1999) 3165.
[13] (a) M.I. Khan, E. Yohannes, R.J. Doedens, Angew. Chem. Int. Ed. 38 (1999) 1292;
(b) M.I. Khan, E. Yohannes, D. Powell, Chem. Commun. (1999) 23;
(c) M.I. Khan, J. Solid State Chem. 152 (2000) 105;
(d) M.I. Khan, E. Yohannes, D. Powell, Inorg. Chem. 38 (1999) 212.
[14] (a) A. Müller, J. Döring, M.I. Khan, V. Wittneben, Angew. Chem. Int. Ed. 30 (1991) 210;
(b) A. Müller, J. Döring, H. Bögge, J. Chem. Soc. Chem. Commun. (1991) 273;
(c) A. Müller, J. Döring, Angew. Chem. Int. Ed. Engl. 27 (1988) 1721;
(d) A. Müller, J. Döring, Z. Anorg. Allg. Chem. 595 (1991) 251.
[15] (a) G.H. Huan, M.A. Greaney, A.J. Jacobson, J. Chem. Soc., Chem. Commun. (1991) 260;
(b) G.Q. Huang, S.W. Zhang, Y.G. Wei, M.C. Shao, Polyhedron 12 (1993) 1483;
(c) E. Dumas, C. Livage, S. Halut, G. Hervé, Chem. Commun. (1996) 243;
(d) S.T. Zheng, J. Zhang, G.Y. Yang, Eur. J. Inorg. Chem. (2004) 2004;
(e) S.T. Zheng, J. Zhang, G.Y. Yang, Inorg. Chem. 44 (2005) 2426.
[16] W.M. Bu, G.Y. Yang, L. Ye, J.Q. Xu, Y.G. Fan, Chem. Lett. (2000) 462.
[17] G.M. Sheldrick, SADABS, University of Göttingen, Göttingen, Germany, 1997.
[18] G.M. Sheldrick, SHELX TL-97, Program for X-ray Crystal Structure Refinement, University of Göttingen, Göttingen, Germany, 1997.
[19] I.D. Brown, D. Altermatt, Acta. Crystallogr. Sect. B 41 (1985) 244.
[20] L.R. Zhang, Z. Shi, G.Y. Yang, X.M. Chen, S.H. Feng, J. Chem. Soc. Dalton Trans. (2000) 275.
[21] V. Soghomonian, Q. Chen, R.C. Haushalter, J. Zubieta, C.J. O'Connor, Science 259 (1993) 1596.
[22] A. Müller, F. Peters, M.T. Pope, D. Gatteschi, Chem. Rev. 98 (1998) 239.
[23] A. Müller, R. Sessoli, E. Krickemeyer, H. Bögge, J. Meyer, D. Gatteschi, L. Pardi, J. Westphal, K. Hovemeier, R. Rohlfing, J. Döring, F. Hellweg, C. Beugholt, M. Schmidtmann, Inorg. Chem. 36 (1997) 5239.
[24] M. Khan, Molecular Magnetism, VCH, Weinhein, Germany, 1993.